

Using FEM for Prediction of Thermal Post-Buckling Behavior of Thin Plates During Welding Process

Amin Esmailzadeh, Mohammad Sadeghi, Farhad Kolahan

Abstract—Arc welding is an important joining process widely used in many industrial applications including production of automobile, ships structures and metal tanks. In welding process, the moving electrode causes highly non-uniform temperature distribution that leads to residual stresses and different deviations, especially buckling distortions in thin plates. In order to control the deviations and increase the quality of welded plates, a fixture can be used as a practical and low cost method with high efficiency. In this study, a coupled thermo-mechanical finite element model is coded in the software ANSYS to simulate the behavior of thin plates located by a 3-2-1 positioning system during the welding process. Computational results are compared with recent similar works to validate the finite element models. The agreement between the result of proposed model and other reported data proves that finite element modeling can accurately predict the behavior of welded thin plates.

Keywords—Welding; Thin Plate; Buckling Distortion; Fixture Locators; Finite Element Modeling

I. INTRODUCTION

WELDING is an important joining process in many industrial products such as automobiles, wagons, ships and metal tanks, large amounts of welded thin plates are used. Welding processes have several advantages over other permanent joining techniques including well sealing, high strength and weight reduction and improved performance of the final structure. However, thin plates welding may result in some geometrical deviations which, in turn, have negative impacts on assembly tolerances and product quality.

The main reasons that cause weldment deviations during welding are the moving heat source, non-uniform temperature distributions and temperature variations [1]. There are several basic types of distortions which may occur during welding of plates. As shown in Fig. 1, they include transverse shrinkage, longitudinal shrinkage, angular, longitudinal bowing, rotational and buckling distortions.

For thin plates, due to low resistance against membrane stresses, buckling distortion is the dominant mode and plays

an important role in distortion control strategies [2]. Furthermore, the positions of fixtures, as boundary conditions of the process, greatly affect the distortions of welded plates [3]. Therefore, using proper fixturing is an effective and low cost solution for welding distortion control.

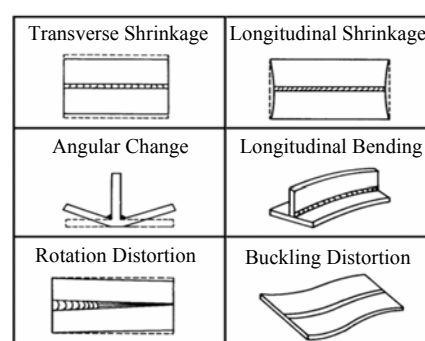


Fig. 1 Basic types of welding distortion

Due to the high flexibility and minimal cost, numerical methods are the most widely used approach to predict welding deviations and residual stresses. Specifically, since mid 70's, Finite Element Method (FEM) is becoming more attractive to simulate various welding processes [4]. In most FEM models, some simplifications have been made. For instance, Hyde [5] simulated thin plates butt welding by a 2D and symmetric model. In several studies, the heat flux in the welding direction is ignored, but Gery [1] reveal shortcomings in this approach. As a solution, Goldak [6] considered the weld heat source has a double ellipse geometry that moves along the welding direction. Researches show that by applying this model, the results would be closer to reality [1, 4, 7]. Because the dimensional changes in welding are negligible, in most present studies the thermo-mechanical behavior of welded plate is simulated using sequentially coupled formulation [8].

In this study, a 2D finite element model is employed to predict the buckling deviation in welded plates. The plates are fixed by 3-2-1 locating system, where the structure of fixture is made of two clamps and one pin. Some assumptions are considered for simplify the fixture modeling. Also a mathematical Goldak's model is used to simulate the welding heat source. The finite element analyses are done in two steps. First, the distribution of temperature in the plates is computed and then the temperature history is employed as a thermal load in the mechanical calculations of post-buckling distortions.

MS Graduated, Department of Mechanical Engineering, Ferdowsi University of Mashhad, Iran (a.esmailzadeh@ymail.com)

MS Student, Department of Mechanical Engineering, Ferdowsi University of Mashhad, Iran (h.sadeghi@ymail.com)

Corresponding Author, Associate Prof., Department of Mechanical Engineering, Ferdowsi University of Mashhad, Iran (kolahan@um.ac.ir)

II. FINITE ELEMENT MODELING OF WELDING

In this study, the welding process for symmetric joining of two thin plates is modeled. As Fig. 2 illustrates, each plate has dimensions of $500 \times 245 \times 1 \text{ mm}^3$ and is located by a fixture including two toggle clamps and one simple pin. The material of plates is mild steel with the ST37 grade [9].

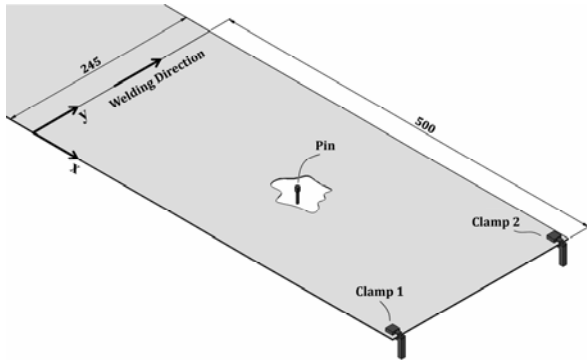


Fig. 2 Moving directions of fixture locators

Since the effect of dimensional changes and mechanical work done on thermal energy from the welding arc are negligible, the thermo-mechanical behavior of the welding can be simulated by sequentially coupled formulation [10]. In other words, the thermal problem is solved independently from the mechanical problem. Hence, the solution procedure consists of two steps: First, the temperature distribution and its history in the welding model are computed using a transient thermal finite elements model. The temperature history is then employed as a thermal load in the mechanical calculations of post-buckling problem. The numerical calculations of thermal and mechanical steps is coded using software ANSYS.

A. Thermal analysis

In this work, a 2D double ellipse power distribution proposed by Golack [6] is used to simulate the moving welding arc. Fig. 3 shows geometry and parameters of the double ellipse model in welding direction (y axis).

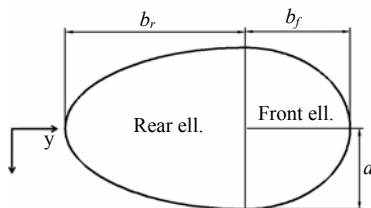


Fig. 3 Double ellipse heat source configuration

Considering geometry of the welding pool, the heat distributions of the front and rear ellipse are obtained from (1) and (2), respectively.

$$q_f(x, y, t) = \frac{6f_f \eta V I}{ab_f \pi} e^{-3x^2/a^2} e^{-3(y-vt-y_0)^2/b_f^2} \quad (1)$$

$$q_r(x, y, t) = \frac{6f_r \eta V I}{ab_r \pi} e^{-3x^2/a^2} e^{-3(y-vt-y_0)^2/b_r^2} \quad (2)$$

Where V , I and η are voltage, current and heat source efficiency, respectively. In addition, distributed heat power in both ellipses is equal to the total power of welding arc ($Q = \eta I V$). Generally temperature gradient at front half of welding pool is steeper than rear half. Hence heat density in two ellipses are given by fractions f_f and f_r of heat deposited, where $f_f + f_r = 2$. In order to simulate moving heat source, a subroutine is coded in software ANSYS. Experimental measurements shows parameters a , b_f and b_r are 5, 3 and 7 mm and fractions f_f and f_r are 1.4 and 0.6, respectively. Also, welding speed, heat source efficiency, voltage and current are considered 4 mm/s, 0.8, 16 V and 65 A, respectively.

In order to simulate the temperature distribution in the welding process using ANSYS codes. The fluid flow and solidification of material in the welding pool cannot be directly considered because the coupled problem between solid and liquid is not involved in FEM software. However, the influence of fluid flow on the temperature distribution is significant. The highest temperature on the molten pool surface is approximately 1750 °C. However, by neglecting the effect of fluid flow, the peak temperature would unusually increase to higher than 3000 °C. This can be resolved using an artificially increased thermal conductivity in the weld pool. The thermal conductivity for temperature above the melting point is assumed to be approximately twice as large as its value of room temperature [10]. Heat losses due to convection and radiation are considered for all the surfaces. Also, a temperature-dependent film coefficient is used to make a more realistic model [8].

B. Mechanical Analysis

In order to create mechanical finite element model, only the element type of thermal model should be changed. The thermal simulation can provide temperature history of welded thin plate. The temperature distribution is considered as thermal load in mechanical simulation.

At first it may seem that a contact analysis between the plate and pin is required, to simulate the pin locator. However, solving nonlinear-eventual problems such as contact analysis is very time consuming. Computational results showed that in-plane sliding distance of plate on pin (Fig. 4) during the welding process is less than 1mm. This value is negligible in comparison to the problem dimensions and out of plane displacements. Therefore, with a reasonable assumption, displacements in x and y directions of node in pin position can be ignored. This node is denoted by \times symbol in Fig. 5.

Generally, fixture structure can be assumed rigid in comparison with the plates. Meanwhile, due to plate weight and dimension of problem, the plate is always laid on the pin. So, pin always stays in contact with plate and restrains vertical displacing of plate, during the welding process. In order to simulate effects of the pin, the out of plane degree of freedom of this node will be inhibited.

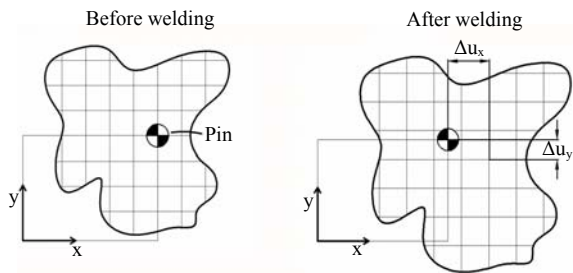


Fig. 4 In-plane displacement of plate on the pin

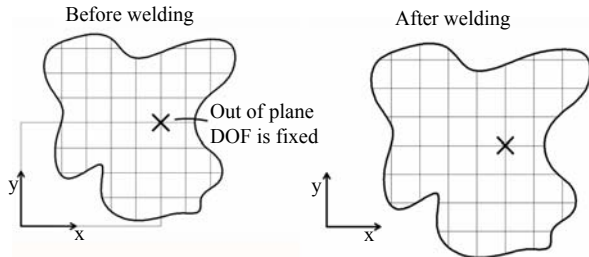


Fig. 5 The simplified assumption for boundary condition of pin

In addition, by clamping, the plate is restrained from displacement in all directions. Therefore, all six node degrees of freedom at clamps positions are restrained from displacement to simulate the clamps.

In this study, distance between two plates is low and transverse shrinkage due to solidification weld pool can be negligible. Thus, considering symmetry of the problem, the x direction displacement of nodes on welding line is inhibited.

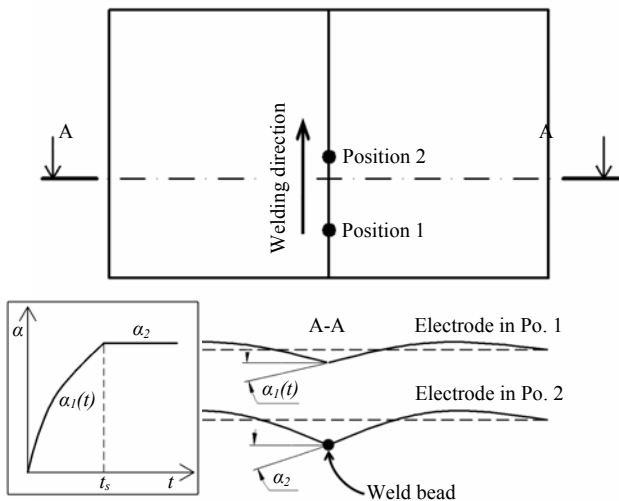


Fig. 6 Plate rotation in welding line area

As Fig. 6 shows, by passing the heat source over the points on welding line and solidification of molten pool, the two plates would be connected together by weld bead creation. This figure also indicates the way of rotation of points around the welding line (y axis).

When the electrode is at position 1, no connection is created between two plates in the middle point of section A-A. Therefore, plates can be rotated freely around the welding line. In this step, plate angle is denoted by $\alpha_1(t)$. After a few

moment, the electrode crosses section A-A and reaches the position 2. By cooling and solidification of molten pool, two plates would be connected together. After weld bead creation, as shown in $\alpha-t$ plot, it can be assumed that plate rotation around the welding line stays in its last value.

In order to simulate the connectivity of two plates, temperature history is investigated to specify the solidification time (t_s) of molten pool. Considering above explanations, before this time, the nodes on welding line can rotate freely around y axis. In this way, the related degree of freedom is kept constant in its last value. Fig. 7 shows the boundary conditions for the symmetry of problem.

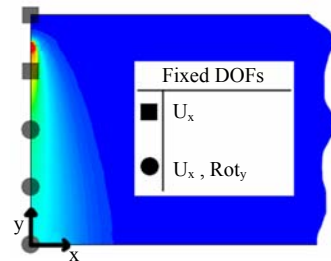


Fig. 7 Boundary condition of two plates connectivity

As mentioned above, the buckling distortion is the dominant mode of thin plate deviations during welding. The buckling problem can be solved by Eigenvalue and nonlinear (large deformation) methods. Eigenvalue buckling analysis predicts the critical buckling load and shape mode of distortion. But using the nonlinear buckling analysis, the measure of distortion can be computed. In this way, the fabrication tolerance and quality of welded plates may be predictable. In this study, the nonlinear buckling analysis is used to predict behavior of weldment.

For the mild steel, influence of phase transformation on welding residual stresses and the distortion is insignificant. The total strain can therefore be decomposed into just three components as follows [8]:

$$\epsilon_{ij} = \epsilon_{ij}^{th} + \epsilon_{ij}^e + \epsilon_{ij}^p$$

Where ϵ_{ij}^{th} , ϵ_{ij}^e and ϵ_{ij}^p are thermal, elastic and plastic strain, respectively.

C. Validation of FEM results

In this section, the results of created FE model will be validated. The results of most works on welding validate by comparison with experimental tests. However, this approach is difficult, costly and time consuming. Therefore, the validation is performed by comparison with recent works.

In order to validate the first step of welding simulation, Deng's [8] results will be compare with thermal results of proposed FE model. For a welded plate having dimensions of $100 \times 100 \times 1 \text{ mm}^3$, Deng predicted temperature history at two points; one on the welding line and the other on the heat affected zone. The comparisons between the present work and

Deng's results are schematically shown in Fig. 8 and Fig. 9. As these figures illustrate the thermal FE model can predict the welding temperature histories with good precision.

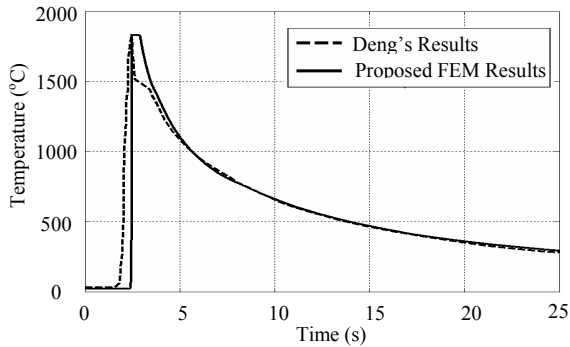


Fig. 8 Comparison of temperature histories at a point on welding line

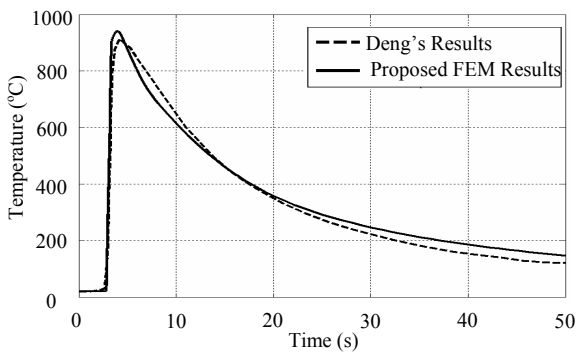


Fig. 9 Comparison of temperature histories at a point on HAZ

The results of proposed mechanical analysis are then compared with similar recent works in the literature. In this regard, Raju's [11] case is simulated by proposed finite element model. He analyzed thermal post-buckling behavior of warmed square plate with simply supported edges using Rayleigh-Ritz method. In order to validate, two cases with uniform and non-uniform temperature distributions, are investigated applying Raju's equations and the proposed FE model. Computational results of two cases are shown in Fig. 10 and Fig. 11. As illustrated, the finite element method has been able to approximate buckling and post-buckling behavior of plates in both cases.

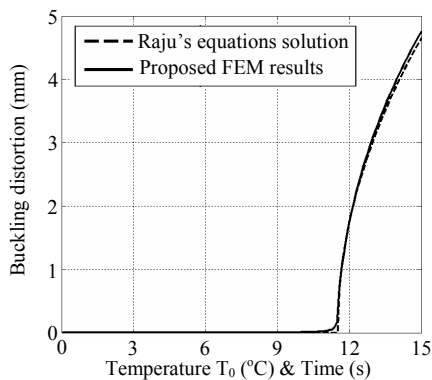


Fig. 10 Validation case with uniform temperature distribution ($T(x,y)=T_0$)

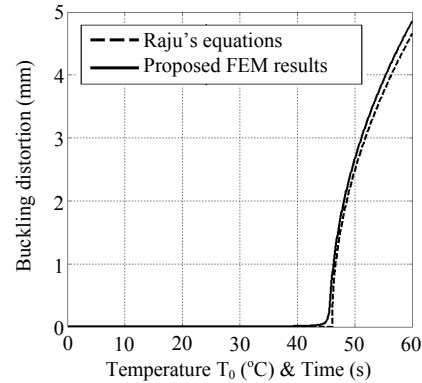


Fig. 11 Validation case with non-uniform temperature distribution ($T(x,y)=T_0(a-x)(a-y)/a^2$)

D. Welding simulation using proposed FE model

In order to discrete the non-linear problem, 10 sets of element size and time stepping is tested. Fig. 12 shows the convergence of distortion measure by different discretion sets. Considering a reasonable solution time, sixth settings including 5300 elements, 2800 nodes and 0.5 s for time step is used in analyses. Fig. 13 represents the applied FE model for welding simulation. The elements of surrounding the locators and welding direction are selected finest, due to stress gradient increases at these areas.

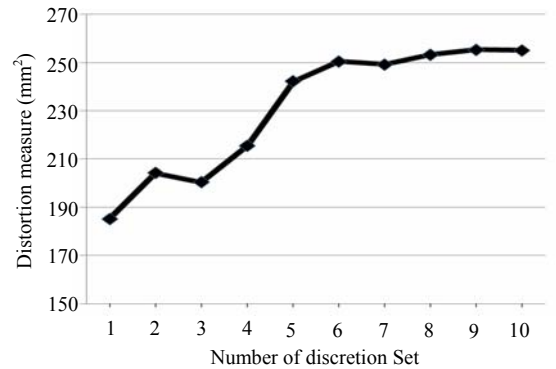


Fig. 12 Mesh sensitivity plot

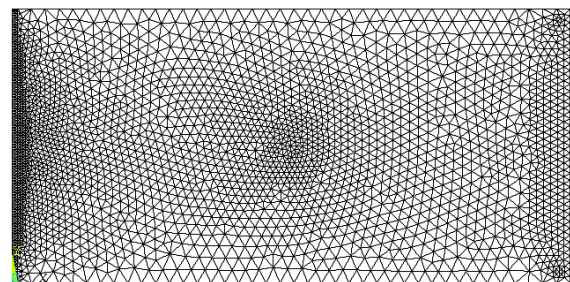


Fig. 13 Plate model used for 2D finite element analyses

By thermal simulating of welded plate, the temperature distribution can also be predicted. Fig. 14 shows the distribution of temperature, 55 second after welding starts. As shown, the peak temperature is at the tip of welding electrode and temperature gradient at the front of electrode is steeper than the rear.

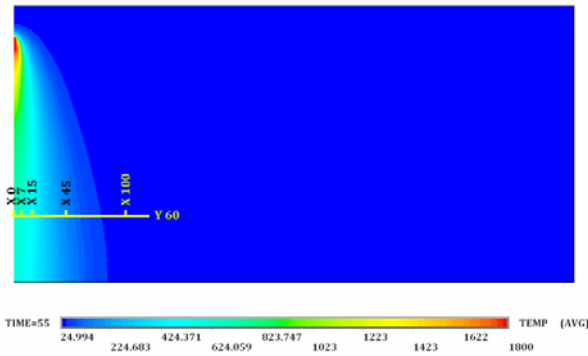


Fig. 14 Temperature distribution of half plate during welding

The temperature at different points of plate is time dependent. As the heat source gets closer, these points have peak temperature and then because of heat losses due to convection the plate will be cooled down to room temperature. Fig. 15 shows the temperature history at some points of Y 60 transverse section.

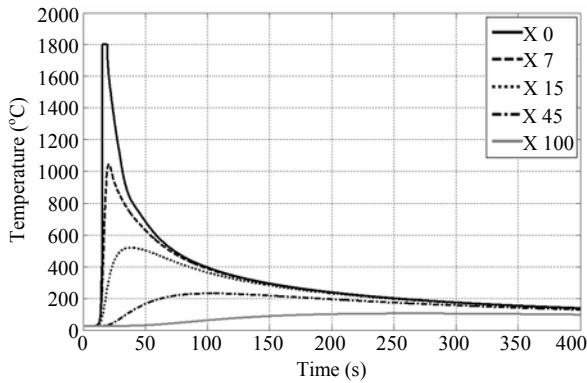


Fig. 15 Temperature histories at points of Y 60 transverse section

By applying the second simulation step, the mechanical behavior of welded can also be predicted. Fig. 16 shows that the measure of distortion at two areas between welding line and pin and between three locators is more than other areas.

Fig. 17 and Fig. 18 shows buckling will certainly occur at these areas. As these figures illustrate, the points close to welding line have been buckled immediately, but buckling occurs at the farther points in later times. Nevertheless, thermal strains at some points have been less than the critical values. For example, in Fig. 18 a point at coordinate of (250, 60) positioned in the transverse direction of pin, is still stable.

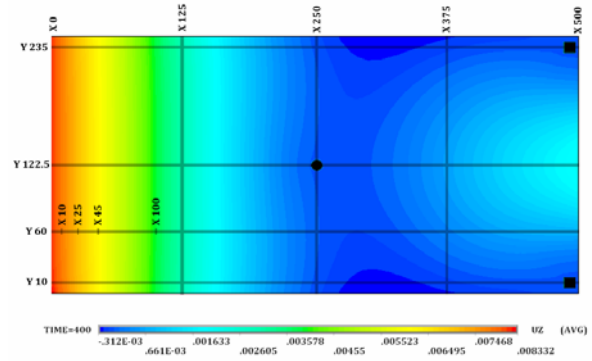


Fig. 16 Post-buckling distortion of one plate during welding

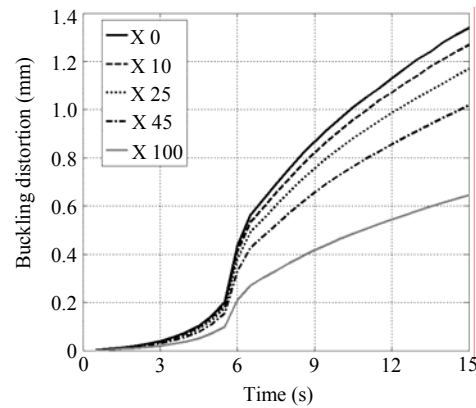


Fig. 17 Distortion histories at points close to welding line on Y 60 transverse section

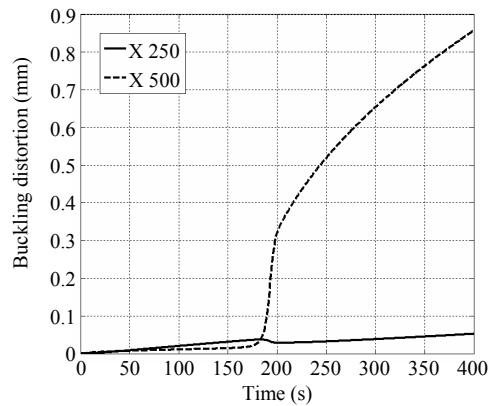


Fig. 18 Distortion histories at points far from welding line on Y 60 transverse section

The buckling mode shape of longitudinal and transverse directions is shown in Fig. 19 and Fig. 20, respectively. It can be seen that because of the large ratio of plate length to width, the buckling occurs only in the longitudinal path at the area between the welding line and the pin. In addition, the pin has been effective in controlling buckling distortion.

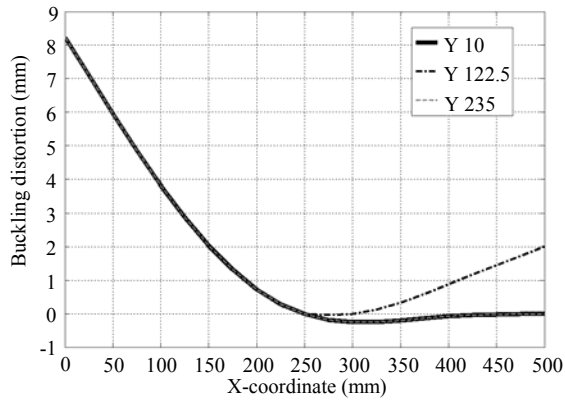


Fig. 19 Longitudinal buckling mode shape of plate in different paths

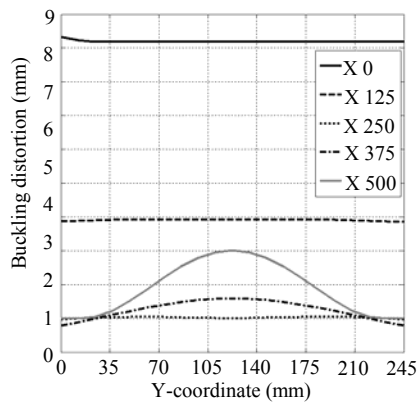


Fig. 20 Transverse buckling mode shape of plate in different paths

III. CONCLUSION

Various welding techniques are widely used as permanent metal joining processes. In welding, the quality of the joint is highly affected by the dimensional inaccuracies due to the welding distortions. Welding distortions may cause geometrical and dimensional inaccuracies in the weldments. In this study, a thermo-elastic-plastic finite element model is used to predict the behavior of welded thin plate during butt welding. The proposed finite element model is close to actual welding process and has few realistic assumptions. In order to validate computational results of the finite element model, comparisons are performed with recently published thermal post-buckling and welding works. Computational results show

that the proposed welding simulation can accurately predict temperature history as well as thermal buckling and post-buckling behaviors in a thin plate during the welding process. In addition, it is shown that proper fixture positions can control the welding distortions with great efficiency.

ACKNOWLEDGEMENT

We highly appreciate Khorasan Razavi Gas Co. for their technical and financial support of this research.

REFERENCES

- [1] D. Gery, H. Long, P. Maropoulos, "Effects of welding speed, energy input and heat source distribution on temperature variations in butt joint welding", *Journal of Materials Processing Technology*, vol. 157, pp. 393-401, 2005.
- [2] C. Conrardy, T. D. Huang, D. Harwig, P. Dong, L. Kvidahl, N. Evans, A. Treaster, "Practical Welding Techniques to Minimize Distortion in Lightweight Ship Structures", *Journal of ship production*, vol. 22, pp. 239-247, 2006.
- [3] J. A. Camelio, S. J. Hu, D. Ceglarek, "Impact of Fixture Design on Sheet Metal Assembly Variation", *Journal of Manufacturing Systems*, vol. 23, pp. 172-193, 2004.
- [4] A. Anca, A. Cardona, J. Risso, V. D. Fachinotti, "Finite element modeling of welding processes", *Applied Mathematical Modeling*, vol. 35, pp. 688-707, 2011.
- [5] T. H. Hyde, A. A. Becker, Y. Song, W. Sun, "Failure estimation of TIG butt-welded Inco717 sheets at 620 °C under creep and plasticity conditions", *Computational Materials Science*, vol. 35, pp. 35-41, 2006.
- [6] J. Goldak, A. Chakravarti, M. Bibby, "A new finite element model for welding heat sources", *Metallurgical Transactions*, vol. 14B, pp. 299-305, 1984.
- [7] T. Schenk, I. M. Richardson, M. Kraska, S. Ohnimus, "A study on the influence of clamping on welding distortion", *Computational Materials Science*, vol. 45, pp. 999-1005, 2009.
- [8] D. Deng, H. Murakawa, "Prediction of welding distortion and residual stress in a thin plate butt-welded joint", *Computational Materials Science*, vol. 43, pp. 353-365, 2008.
- [9] Z. Barsoum, I. Barsoum, "Residual stress effects on fatigue life of welded structures using LEFM", *Engineering Failure Analysis*, vol. 15, pp. 449-467, 2009.
- [10] D. Deng, "FEM prediction of welding residual stress and distortion in carbon steel considering phase transformation effects", *Materials and Design*, vol. 30, pp. 359-366, 2009.
- [11] K. K. Raju, G. V. Rao, "Thermal post-buckling of thin simply supported orthotropic square plates", *Composite Structures*, vol. 12, pp. 149-154, 1989.